Maternal nutrition modifies trophoblast giant cell phenotype and fetal growth in mice

Adam J. Watkins[1, 2], Emma S. Lucas[1], Stephanie Marfy-Smith[1], Nicola Bates[3], Susan J, Kimber[3], and Tom P. Fleming[1]

[1]Centre for Biological Sciences, University of Southampton, Southampton General Hospital, Southampton SO16 6YD, United Kingdom.

[2]Aston Research Centre for Healthy Ageing, School of Life and Health Sciences, Aston University, Birmingham, B4 7ET, United Kingdom.

[3]Faculty of Life Sciences, University of Manchester, Michael Smith Building, Oxford Road, Manchester, M13 9PT. United Kingdom.

Corresponding Author:

Adam J. Watkins: Aston Research Centre for Healthy Ageing, School of Life and Health Sciences, Aston University, Birmingham, B4 7ET, United Kingdom.

E mail: a.watkins1@aston.ac.uk

Short Title: Maternal diet and trophoblast phenotype

Mammalian placentation is dependent upon the action of trophoblast cells at the time of implantation. Appropriate fetal growth, regulated by maternal nutrition and nutrient transport across the placenta, is a critical factor for adult offspring long-term health. We have demonstrated that a mouse maternal low protein diet (LPD) fed exclusively during preimplantation development (Emb-LPD) increases offspring growth but programmes adult cardiovascular and metabolic disease. Here, we investigate the impact of maternal nutrition on post-implantation trophoblast phenotype and fetal growth. Ectoplacental cone explants were isolated at day 8 of gestation from female mice fed either normal protein diet (NPD: 18% casein), LPD (9% casein) or Emb-LPD and cultured in vitro. We observed enhanced spreading and cell division within proliferative and secondary trophoblast giant cells (TGCs) emerging from explants isolated from LPD females when compared with NPD and Emb-LPD explants after 24 and 48 hours. Moreover, both LPD and Emb-LPD explants showed substantial expansion of TGC area during 24 to 48 hours, not seen in NPD. No difference in invasive capacity was observed between treatments using Matrigel transwell migration assays. At day 17 of gestation, LPD and Emb-LPD conceptuses displayed smaller placentas and larger fetuses respectively, resulting in increased fetal:placental ratios in both groups compared to NPD conceptuses. Analysis of placental and yolk sac nutrient signalling within the mTORC1 pathway revealed similar levels of total and phosphorylated downstream targets across groups. These data demonstrate that early post-implantation embryos modify trophoblast phenotype to regulate fetal growth under conditions of poor maternal nutrition.

Introduction

The development of the mammalian fetus is fundamentally dependent upon successful implantation of the embryo into the uterine tissue. This essential step is regulated by the action of the trophoblast cells which coordinate the complex processes of embryo attachment and implantation, uterine spiral artery remodelling and initiate the development of the placenta. At the time of implantation, the embryo is comprised of two distinct cell lineages, the inner cell mass (ICM) containing the progenitor cells of the fetal and primitive endoderm lineages, and the trophectoderm (TE) comprising the progenitors of the chorio-allantoic placenta. Following implantation, trophectoderm cells not in direct contact with the ICM (mural trophectoderm) exit mitosis, endo-reduplicate their DNA and give rise to the primary trophoblast giant cells (TGCs). These primary TGCs form blood sinuses at the periphery of the embryo, contributing to the provision of nutrients and oxygen to the developing embryo by the yolk sac (Bevilacqua and Abrahamsohn 1988). In contrast, the trophectoderm cells directly overlying the ICM (polar trophectoderm) differentiate into the chorion and ectoplacental cone (EPC), from which secondary TGCs are derived (Simmons and Cross 2005).

The large polyploid secondary TGCs invade into the maternal decidual tissue and spiral arteries to establish maternal-fetal nutrient transfer (Adamson, et al. 2002) as well as secreting a range of hormones and cytokines which modulate the maternal uterine environment, both essential for fetal growth (Simmons, et al. 2007, Soares, et al. 2007). At around day 8.5 of gestation in the mouse (E8.5), the allantois begins to attach to the chorion initiating the formation of both the junctional and labyrinth zones of the developing placenta. Ultimately, the labyrinth zone will mediate nutrient exchange between the fetus and mother through a highly developed vascular network, whilst the junctional zone becomes the site of growth factor and pregnancy-related hormone production (Georgiades, et al. 2002). Therefore, disruption to the normal process of trophoblast differentiation or phenotype specification during early gestation (E8.5) is likely to affect detrimentally embryo viability, placental morphology and function and ultimately fetal growth and development.

Over recent decades, the regulation of fetal growth and development has become of significant interest in light of human epidemiological and animal model observations demonstrating links between altered fetal growth and predisposition to adult-onset cardiovascular and metabolic disease (Hanson and Gluckman 2014). The significant similarities between human and rodent preimplantation embryo development, implantation and placental morphology means mice and rats provide biologically applicable models with which to investigate the sensitivity of the developing placenta and its impact on offspring health. In mice, maternal caloric restriction results in differential placental expression of genes associated with intra-uterine growth restriction and genome wide hypomethylation (Chen, et al. 2013), whilst a high fat diet induces sex-specific changes in placental gene expression for immune and inflammatory responses and regulators of epigenetic modifications (Gabory, et al. 2012). Changes in placental gene expression within apoptosis, growth inhibition and epigenetic modification pathways have also been observed in response to a maternal low protein diet in mice (Gheorghe, et al. 2009), whilst in the rat, changes in placental mammalian Target of Rapamycin complex 1 (mTORC1) and amino acid transporter protein levels have been demonstrated (Rosario, et al. 2011). Additional changes in placental structure, nutrient transport, and fetal cytokine levels have also been reported in response to maternal dietary manipulation (Armitage, et al. 2004, Chen, et al. 2013, Coan, et al. 2011, Kim, et al. 2014, Sferruzzi-Perri, et al. 2013).

We have shown that a maternal low protein diet (LPD; 9% casein) fed to mouse dams exclusively during preimplantation development (days 0-3.5 of gestation; Emb-LPD) enhances postnatal growth and adiposity and induces hypertension, vascular dysfunction and altered behavioural characteristics in adult offspring (Watkins, et al. 2010, Watkins, et al. 2011, Watkins, et al. 2008). We observed additionally that enhanced early postnatal growth was a significant predictor of adult adiposity, cardiovascular health and behaviour (Watkins, et al. 2008). Blastocysts

transferred from LPD fed dams into recipient NPD fed dams displayed elevated fetal growth, when assessed at E17, demonstrating that offspring programming is initiated during preimplantation development (Watkins, et al. 2008). Analysis of embryonic and extraembryonic lineage tissues from Emb-LPD dams has revealed elevated blastocyst TE:ICM ratio and differential signalling through the mTORC1 nutrient sensing pathway (Eckert, et al. 2012), enhanced endocytic and lysosomal activity within blastocyst trophectoderm and embryoid body primitive endoderm (Sun, et al. 2014) and enhanced uptake and transport capacity within the late gestation visceral yolk sac (Watkins, et al. 2008). From these data, we propose that the preimplantation embryo senses the maternal uterine nutritional status directly and initiates a series of adaptive mechanisms within the extraembryonic lineages to enhance nutrient uptake and maintain growth. However, upon restoration of an optimal maternal nutrition post-implantation, these enhanced nutrient uptake adaptations become maladaptive, promoting increased felt growth and adult offspring ill-health.

Whilst the impact of maternal diet on embryonic and late gestation placental nutrition-uptake mechanisms have been investigated in detail, the nutritional impacts on early post-implantation dynamics, and how these processes influence the development of the mature placenta, remain unknown. Therefore, in the current study, we have extended our mouse gestational dietary model to investigate for the first time the impact of Emb-LPD on early post-implantation trophoblast giant cell phenotype *in vitro*, late gestation fetal growth and placental development.

Materials and Methods

Animal Treatments

All mice and experimental procedures were conducted using protocols approved by, and in accordance with, the UK Home Office Animal (Scientific Procedures) Act 1986 and local ethics committee at the University of Southampton. Virgin female MF-1 mice (aged 7-8.5 weeks), derived

within the University's Biomedical Research Facility, were maintained on a 07:00–19:00 light-dark cycle at a temperature of 20–22°C and fed *ad libitum* on standard laboratory chow (Special Diet Services Ltd, UK), were housed singly overnight with MF-1 studs. The presence of a vaginal plug the following morning was taken as a sign of mating. Plug positive females were housed singly and allocated randomly to one of three isocaloric (calories/g; Special Dietary Services Ltd, UK; composition published previously, (Watkins, et al. 2011)) dietary regimens; (1) normal protein diet (NPD; 18% casein, 42.5% maize starch, 21.3 % sucrose, 10% corn oil, 5% cellulose), (2) low protein diet (LPD; 9 % casein, 48.5 % maize starch, 24.3% sucrose, 10% corn oil, 5% cellulose) or, (3) LPD from detection of a vaginal plug until day 3.5 of gestation then switched to NPD for the remainder of gestation (Emb-LPD). Females were culled via cervical dislocation at either E8.5, for the isolation and culture of postimplantation ectoplacental cones (EPCs), or at day 17 (E17) for analysis of fetal growth and placental and yolk sac mTORC1 signalling.

Isolation of ectoplacental cone explants

In the mouse, E8.5 represents a developmental stage during which trophoblast differentiation and early placental lineage induction is being established. Therefore, analysis of EPC outgrowth phenotype at this stage could provide significant insight into the establishment of the mature placenta and the regulation of fetal growth in response to maternal diet (El-Hashash and Kimber 2004, El- Hashash, et al. 2005). At E8.5, NPD, LPD and Emb-LPD dams were culled by cervical dislocation. Whole uteri were excised and placed within pre-warmed (37 ^{o}C) Dulbecco's modified Eagles' medium (DMEM; Life Technologies, Paisley, UK) with 10 % (v/v) heat inactivated fetal calf serum (Sigma Aldrich, Poole, Dorset, UK). Individual decidual capsules were dissected from both uterine horns prior to isolation of whole embryos from within the surrounding decidual tissue. Ectoplacental cones (EPCs) were separated from the embryo at the junction with the extraembryonic ectoderm using sterile fine forceps.

Culture and outgrowth of secondary trophoblast giant cells

Previously, we have demonstrated increased TE cell number and *in vitro* outgrowth expansion in blastocysts collected from LPD fed dams (Eckert et al., 2012). To determine whether similar increases in expansive phenotype were still present within EPC outgrowths at E8.5, we cultured explants on cover slips to assess their growth within a 2-dimensional plane. This approach enabled us to determine migratory phenotype whilst maintaining the close architectural structure of the outgrowth and preserving cell-cell contacts. Sterile cover slips were coated with BD Matrigel™ basement membrane matrix (BD Biosciences, UK) diluted to 6 mg/ml in RPMI 1640 medium (Life Technologies, UK) and left at 4 ^{o}C overnight in 4-well plates (Sigma Aldrich, UK). The following morning, the Matrigel-RPMI medium was replaced with 500 µl sterile filtered RPMI 1640 medium (Life Technologies, UK) containing 2 % KnockOut™ Serum Replacement (Life Technologies, UK), penicillin-streptomycin-glutamine mix (Life Technologies, UK) and 26.2 µmol 2-mercaptoethanol (Sigma Aldrich, UK) and allowed to equilibrate at 37 ^{o}C, 5 % CO_2 in air for at least one hour. Dissected EPC explants were cultured individually at 37 ^{o}C, 5 % CO_2 in air for up to 48 hours with a 50 % medium change after 24 hours.

Assessment of EPC explant invasive capacity

As well as cell migration, cell invasion is an important event in the development of the placenta. To obtain a greater understanding of the invasive capacity of outgrowths we cultured EPC explants on Matrigel transwell inserts. Using this approach, we could quantitate invasive and migratory capacity through a 3-dimensional membrane, replicating more closely an *in vivo* environment when compared with cover slips. Matrigel invasion assays of EPC explants were performed using BD BioCoat Matrigel Invasion Chambers (VWR, Lutterworth, UK). Transwell inserts (8 µm pore size) were re-hydrated within a 24 well plate with RPMI 1640 medium (Life Technologies, UK) (500 µl per well and per insert) at 37 ^{o}C, 5 % CO_2 for 2 hours after which the medium was replaced with RPMI medium containing serum replacement, penicillin-streptomycin-glutamine and 2-

mercaptoethanol (as above; 750 µl within the well and 500 µl within the invasion chamber). Invasion chambers were allowed to equilibrate at 37 ^{o}C, 5 % CO_2 in air for at least one hour. EPC explants, isolated as described above, were cultured singly per well for up to 48 hours with a 50 % medium change after 24 hours.

Morphological and invasive analysis of outgrowths

EPC outgrowths, both on coverslips and invasion chambers, were fixed after 24 or 48 hours of culture in 4 % neutral buffered formalin (Sigma Aldrich, UK) for 15 minutes prior to permeabilisation with 0.1 % Triton-X100 (Sigma Aldrich, UK) for 5 minutes, and washed three times with PBS at room temperature. Background staining was minimised with ammonium chloride (2.6 mg/ml in PBS) for 10 minutes prior to an additional 5 minute permeabilisation step (0.1% Triton-X100) and PBS washing, all conducted at room temperature. Non-specific binding was blocked with 2 % BSA in PBS containing 0.1 % Triton-X100 for 30 minutes at room temperature prior to overnight incubation at 4 ^{o}C with primary antibody for alpha tubulin (1:2000; Cell Signaling, Danvers, United States of America) in PBS with 1% BSA and 0.1 % Triton-X100. Following PBS-0.1 % Triton-X100 washes, outgrowths were incubated with the appropriate Alexa Fluor conjugated secondary antibody (1:10,000; Molecular Probes, Life Technologies, UK) for 1 hour at room temperature and counter- stained for nuclei using DAPI (Sigma Aldrich, UK) for 10 minutes prior to mounting on slides in DPX (Fisher, Loughborough, UK). All outgrowths were imaged using a Leica DSM 5000 microscope with epifluorescence capacity and analysed using Volocity software. The central EPC was defined as the central, single mass within which individual cell nuclei could not be determined. Proliferative trophoblast nuclei were defined as located within the proximity of the central EPC and having a nuclear area < 300 µm^2 (El-Hashash and Kimber 2004, Scott, et al. 2000). Secondary trophoblast were defined as being located at the periphery of the outgrowth and possessing a nuclear area > 300 µm^2 (El-Hashash and Kimber 2004). Each outgrowth was assessed for the area of the EPC, proliferative and secondary trophoblast cells and of

the whole outgrowth; distance of furthest nucleus from the centre of the EPC; perimeter of the outgrowth and number of secondary trophoblast cells.

Analysis of fetal growth

At E17, NPD, LPD and Emb-LPD dams were culled for the analysis of fetal growth. Whole uteri were removed, placed in ice cold PBS and the number of conceptuses per horn recorded. Individual concepti were dissected carefully from the uterine tissue and weighed prior to separation of the fetus from the placenta and yolk sac. Each fetus, placenta and yolk sac was weighed individually prior to decapitation of the fetus for the collection of serum. Isolated placentae and yolk sacs were snap frozen in liquid nitrogen ahead of protein level analysis.

Placental and yolk sac mTOR analysis

Individual placentae and yolk sacs were homogenised in lysis buffer (50 mM HEPES pH 7.4, 150 mM NaCl, 1 mM EDTA, 1 mM EGTA, 1 % NP40; Sigma Aldrich UK) containing 2% v/v protease inhibitor (cOmplete mini protease inhibitor cocktail, Roche, Burgess Hill, UK) and 1% v/v phosphatase inhibitor cocktails 1 and 2 (Sigma Aldrich, UK). Protein levels were determined using the DC protein assay kit (Bio-Rad, Hemel Hempstead, UK) prior to boiling in LDS sample buffer (Life Technologies, UK) and running on 4-12% bis-tris gels (Life Technologies, UK). Proteins were transferred to nitrocellulose membranes overnight, blocked in 5 % milk in TBS-Tween (0.1 % Tween 20; Sigma Aldrich, UK) before incubation overnight at 4 °C with primary antibodies (Cell Signaling) for total 4E-BP1 (1: 1000), phospho- (Thr37/46) 4E-BP1 (1:1000), total S6 ribosomal protein (1:2000), phospho- (Ser235/236) S6 ribosomal protein (1:2000) and α-tubulin (1:10,000) all diluted in 5 % BSA in TBS-Tween. After overnight incubation, membranes were washed in TBS-Tween prior to 1 hour incubation with appropriate species-specific, IRDye-conjugated secondary antibodies (Rockland; Pennsylvania, USA) in 5 % milk in TBS-Tween^{TM} 20 at room temperature. Following additional washes with TBS-Tween^{TM} 20, membranes were analysed by densitometry

using an Odyssey Infrared Imaging System (Licor). Proteins of interest were normalised to α-tubulin to control for differences in total protein loaded.

Statistical analysis

All data was assessed for normality using the Shapiro-Wilk normality test (SPSS 21). All fetal offspring organ weight data were analysed using a multilevel random effects regression model (SPSS version 21) to account for maternal origin of litter, gestational litter size, offspring sex and body weight where appropriate (Watkins, et al. 2008). Analysis of placental and yolk sac protein levels and all EPC outgrowth measurements was conducted using univariate ANOVA with Tukey's multiple comparison post hoc test for normally distributed data, or a Kruskal-Wallis test with Dunn's multiple comparisons post hoc test for non-normally distributed data (SPSS 21). Where possible, all data were assessed for interactions between maternal diet, offspring sex and litter size. Significance was taken at $P<0.05$.

Results

Characterisation of EPC explant outgrowth on Matrigel coated cover slips

At the time of cull (E8.5), the mean number of implantation sites per female (10.53 ± 0.39) and the mean cross section area of EPCs isolated for culture either on cover slips or in transwell inserts (0.83 ± 0.04 mm^2) did not differ between treatment groups ($P >0.2$). We first assessed the outgrowth characteristics of isolated EPC explants on cover slips coated with the basement membrane matrix Matrigel. After 24 hours in culture, explants were observed to form a diffuse outgrowth, radiating in all directions from the central EPC. Visual inspection of outgrowths revealed them to be comprised of two populations of cells; those immediately surrounding the central EPC which appeared small, densely packed and with elongated nuclei, and those at the periphery which were larger and possessed more rounded nuclei (Fig. 1a). After 48 hours,

outgrowths had increased in size but still comprised a central EPC surrounded immediately by small densely packed cells with larger cells populating the periphery (Fig. 1, b, c and d). Closer examination of these cell populations revealed the outer cells to be large (> 1000 μm^2), flat and multi-nucleated whist those cells surrounding the central EPC appeared smaller, multi-layered and possessed a single nucleus (Fig. 1e, f). Previous studies have identified the cells closest to the central EPC explant as being proliferative stem cells (El-Hashash and Kimber 2004, Scott, et al. 2000), whilst those cells located at the outgrowth periphery display morphological characteristics of TGCs (large, multinucleated, single layered) and express specific markers such as PL-II, not expressed within proliferating cells (El-Hashash and Kimber 2004).

Using these morphological characteristics, we defined mean fluorescence intensity (alpha tubulin) and nucleus area (DAPI) threshold values to define the area of the central EPC (Fig. 2a). To determine the distance of the furthest nucleus from the centre of the EPC, a square boundary encompassing the entire highlighted EPC was superimposed and the centre of this square determined by 2 diagonal lines connecting each corner. From the crossing point of these 2 lines, the distance of the furthest nuclei could be determined (Fig. 2b). In addition, we determined the area of proliferative (Fig. 2c) and secondary TGCs as well as the total area and perimeter of each outgrowth. These standardised threshold values were then applied to each outgrowth image to provide an objective set of measurement criteria. Analysis of EPC explants after 24 hours revealed LPD outgrowths had a significantly larger mean total area (i.e. comprising central EPC and surrounding proliferative and secondary TGCs) than NPD outgrowths ($P = 0.05$) and a trend to exceed that of Emb-LPD outgrowths ($P = 0.092$) (Fig. 2d). Both LPD and Emb-LPD outgrowths had significantly increased mean EPC area after 24 hours when compared to NPD outgrowths (Fig. 2e) ($P < 0.01$). No differences in mean area of proliferative or secondary TGCs, or in their combined area, were observed between groups after 24 hours (Fig. 2f-h). However, Emb-LPD outgrowths had significantly reduced mean number of secondary TGC nuclei when compared to NPD and LPD

outgrowths (Fig. 2i) ($P < 0.01$). Despite no significant difference in mean distance of the furthest cell from the centre of the EPC being observed between groups (Fig. 2j) LPD outgrowths displayed an increased outgrowth perimeter when compared to NPD and Emb-LPD outgrowths (Fig. 2k) ($P < 0.05$).

After 48 hours of culture on Matrigel coated cover slips, LPD outgrowths displayed significantly elevated mean total outgrowth area (Fig. 2d), EPC area (Fig. 2e), area of secondary TGCs (Fig 2g), combined proliferative and secondary TGC area (Fig. 2h), number of secondary TGC nuclei (Fig. 2i), distance of furthest nucleus from the EPC centre (Fig. 2j) and outgrowth perimeter (Fig. 2k) when compared to outgrowths from both NPD and Emb-LPD females ($P < 0.05$). Outgrowths from Emb-LPD fed females displayed a significantly reduced mean area of proliferative cells when compared to outgrowths from NPD females after 48 hours (Fig. 2f) ($P = 0.006$) and at a trend level ($P = 0.074$) when compared to LPD outgrowths.

Using data collected on outgrowth proportions for each dietary group between 24 and 48 hours in culture, we assessed the relative development and changes in EPC, proliferative and secondary TGC composition. After 24 hours of culture on Matrigel coated cover slips, outgrowths from Emb-LPD females were composed of a significantly higher EPC and reduced secondary TGC proportion when compared to outgrowths from NPD females (Fig. 3a) ($P < 0.05$). After 48 hours of culture, no significant differences in mean EPC or secondary TGC proportions were observed between groups (Fig. 3b). However, significantly reduced proliferative TGC proportions were observed for outgrowths from females fed LPD and Emb-LPD when compared to NPD females (Fig. 3b) ($P < 0.05$). This alteration in outgrowth composition between 24 and 48 hours of culture resulted from significant reductions in mean EPC proportions (LPD 11.99 %, Emb-LPD 12.20 %) and increased secondary TGC proportions (LPD 14.50 %, Emb-LPD 15.49 %) whilst the NPD outgrowths altered their EPC and secondary TGC proportions by 1 % or less (Fig. 3c).

Characterisation of EPC explant invasive phenotype

In addition to our analysis of EPC explant outgrowth on cover slips, we also assessed explant invasive capacity *in vitro* using Matrigel coated transwell inserts. After 6 hours we observed that relatively few cells had penetrated the Matrigel coating, migrating through the 8 µm pores (Fig. 4a) and spreading over the under-surface of the insert (Fig. 4b). The number of cells observed to have migrated to the under-surface of the insert increased between 12 hours (Fig. 4c) and 24 hours (Fig. 4d) such that, following 24 hours in culture, a large population of cells were present on the under surface of the insert. Closer examination of these invasive and migratory cells after 24 hours of culture revealed a central mass of densely packed, predominately mono-nucleated cells, with a single layer of larger, multinucleated cells at the periphery (Fig. 4e, f), reflective of outgrowths cultured on coverslips. After 36 hours of culture, the large number of cells present on the under-surface of the insert prevented identification of individual nuclei and therefore, quantitative determination of cell migration and outgrowth invasive characteristics (data not shown). Therefore, we analysed outgrowth invasive phenotype after 18 and 24 hours of culture, measuring total outgrowth area and perimeter, number of nuclei and distance of furthest nuclei from the centre of the outgrowth.

After 18 hours in culture, no significant difference in mean outgrowth area, number of nuclei, distance of furthest nucleus, outgrowth area per nucleus or perimeter was observed between treatment groups (Fig. 4g-k). After 24 hours in culture, Emb-LPD outgrowths displayed a significantly reduced mean distance of furthest nucleus from the outgrowth centre (Fig. 4i; $P = 0.017$) and reduced mean outgrowth area and perimeter at trend levels (Fig. 4g, e; $P < 0.01$).

Fetal development at E17

Previously, we have demonstrated elevated fetal growth at E17 in offspring derived from blastocysts transferred from LPD into NPD fed dams (Watkins et al., 2008). This significantly increased growth reflected weight at birth and throughout life of Emb-LPD offspring. Therefore, to determine if maternal diet influenced fetal development in the current study, we evaluated fetal growth at the same stage (E17) of gestation (Table 1). At the time of cull (E17) there was no significant difference in mean litter size between treatment groups (NPD 12.86 ± 0.95, LPD 13.31 ± 0.37, Emb-LPD 11.15 ± 0.50; $P > 0.05$). Concepti from Emb-LPD dams were significantly heavier than those from NPD and LPD dams ($P < 0.05$). Following dissection, Emb-LPD fetuses also displayed elevated weight when compared to NPD and LPD fetuses ($P < 0.05$). Placentas from LPD fetuses were significantly lighter than those of NPD and Emb-LPD fetuses ($P < 0.05$). The significantly increased Emb-LPD fetal weight and decreased LPD placental weight resulted in significant increased fetal:placental ratios in both groups when compared to NPD offspring. Despite no difference in mean yolk sac weight being observed between dietary groups, Emb-LPD fetuses displayed a significantly elevated fetal:yolk sac ratio when compared to NPD and LPD fetuses ($P < 0.01$).

E17 placental and yolk sac mTOR protein analysis

Changes in placental size, function and mTORC1 activity in response to maternal gestational diet have been demonstrated previously (Jansson, et al. 2012, Rosario, et al. 2011). Therefore, we assessed the total and phosphorylated levels of the downstream targets of mTORC1, 4E-BP1 and S6 ribosomal protein, in placental and yolk sac tissues. 4E-BP1 acts as a translation repressor protein by binding to the translation initiation factor eIF4E, an interaction inhibited by the phosphorylation of 4E-BP1 (Dowling, et al. 2010). Conversely, the phosphorylation of S6 ribosomal protein, mediated by phosphorylated S6 kinase, results in the translation of terminal oligopyrimidine (TOP)-dependent transcripts, encoding ribosomal proteins involved in cell cycle progression and translation regulation (Kim 2009). Analysis of total and phosphorylated 4E-BP1 and S6 ribosomal

protein levels in offspring placental and yolk sac tissue revealed no significant differences between treatment groups (Figure 5). However, a trend towards a reduced level of phosphorylated 4E-BP1 and a decrease in the ratio of phosphorylated to total 4E-BP1 in LPD placentas was observed when compared to NPD placentas (P = 0.077 and 0.099 respectively). Similarly, decreased levels of total and phosphorylated S6 ribosomal protein were observed in LPD placentas when compared to NPD and Emb-LPD placentas, though these did not reach significance. No differences were observed in the levels of 4E-BP1 or S6 ribosomal protein in offspring yolk sac tissue between dietary groups.

Discussion

Appropriate placental development and function plays a pivotal role in directing fetal growth, offspring phenotype and influencing adult predisposition to cardiovascular and metabolic disease risk (Vaughan, et al. 2011). During early mammalian development, trophoblast giant cells (TGCs) are fundamental for the establishment of maternal-fetal nutrient and gas exchange and in the formation of the placenta (Rossant and Cross 2001). As the post-implantation ectoplacental cone (EPC) is considered the primary source of secondary TGCs, the *in vitro* culture of the EPC provides a system in which early placental dynamics can be assessed in response to maternal nutritional status. In the present study, we investigated the impact of maternal low protein dietary regimes on post-implantation trophoblast spreading phenotype and invasive capacity *in vitro*, fetal development and signalling through the nutritional sensing mTORC1 pathway in late gestation placenta and yolk sac tissues. We observed that maternal LPD enhanced the development and growth of EPC explants taken at E8.5, but that their invasive capacity remained unaltered when compared to explants taken from NPD and Emb-LPD dams. In late gestation (E17), both maternal LPD and Emb-LPD treatments induced significant increases in fetal:placental ratio, through reduced placental and enhanced fetal growth respectively. Signalling responses mediated by the mTORC1 pathway within the placenta and yolk sac tissues were similar across all treatment groups. These results expand our

386 understanding of the early developmental mechanisms regulating fetal growth and development in
387 response to maternal nutrition, providing novel insight into the programming of adult offspring
388 health.
389
390 Mouse TGC differentiation has been characterised in detail, revealing a complex expression pattern
391 of blood groups antigens (B and Le-b/Le-y) integrins (α_7), hormones (PL-II, PTHrP) and
392 transcription factors (AP-2γ) both *in vitro* and *in vivo* (Auman, et al. 2002, Brown, et al. 1993,
393 Centrella, et al. 1989, El-Hashash, et al. 2010). It has been demonstrated that cells with large
394 nuclear area (>300μm^2) located at the periphery of EPC outgrowths express PL-II and AP-2γ,
395 identifying these as secondary trophoblast giant cells (El-Hashash and Kimber 2004). In contrast,
396 cells located immediately adjacent to the EPC have been shown to be proliferative stem cells (Scott,
397 et al. 2000). Therefore, using these pre-defined morphological (cell size, nuclear area, single or
398 multi-layered) and locational (peripheral or adjacent to the EPC) characteristics, we quantitatively
399 measured EPC explant outgrowth *in vitro*. EPC explants from all treatments groups outgrew in a
400 radial fashion, retaining a central EPC mass surrounded by small, dense, round proliferative cells.
401 At the periphery of each outgrowth were large, flat, multinucleated cells. Upon quantification of
402 each of these outgrowth regions we observed that EPC explants cultured from LPD fed dams
403 displayed significantly 7larger EPC and secondary TGC areas with increased numbers of secondary
404 TGC nuclei when compared to NPD and Emb-LPD outgrowths after 24 and 48 hours. The increase
405 in secondary TGC area appeared driven by increased rates of cell division, as indicated by an
406 increased number of nuclei. However, a disproportionate increase in the number of large multi-
407 nucleated secondary TGCs in LPD outgrowths cannot be discounted. In addition, the contribution
408 of cells from the proliferative region was not assessed, and so an increase in cell allocation from this
409 area cannot be dismissed. However, as no significant differences in mean proliferative TGC area
410 were observed, the contribution to the increase in secondary TGC area may be small. Interestingly,
411 we observed modest increases in EPC outgrowth in both NPD and Emb-LPD explants, differing

from each other in EPC area (increased in Emb-LPD) and number of secondary TGCs (decreased in Emb-LPD) at 24 hours only. Therefore, the up-regulation of EPC outgrowth phenotype in response to maternal LPD could provide a more metabolically efficient early gestation adaptive mechanism to promote enhanced embryonic-maternal vascular connection and maintain fetal development rather than increasing placental mass in late gestation. Indeed, changes in extra-embryonic lineage allocation and spreading phenotype have been identified in blastocysts collected from LPD fed mouse and rat dams (Eckert, et al. 2012, Kwong, et al. 2000). In addition, enhanced endocytotic and lysosomal activity within LPD blastocyst trophectoderm and embryoid body primitive endoderm has also been reported (Sun, et al. 2014). Similar adaptive responses have been shown to occur in response to maternal diabetes where enhanced rates of cell proliferation have been reported in EPCs and late gestation placentas collected from diabetic rat dams, whilst the culture of control dam EPCs in high glucose media increased rates of EPC spreading (Caluwaerts, et al. 2000, Zorn, et al. 2011).

To determine whether maternal diet affected outgrowth invasive capacity, we cultured isolated EPCs on Matrigel coated porous membranes, allowing invasive cells to penetrate the gel and migrate to the lower surface. Matrigel assays have been used to characterise the invasive phenotype of human trophoblast cells (O'Brien, et al. 2003, Sato, et al. 2002, Xu, et al. 2002), revealing differential invasive responses to a range of pro-inflammatory cytokines (Bauer, et al. 2004, Jovanovic, et al. 2010, Pavan, et al. 2004, Staff, et al. 2000). In mouse assays, trophoblast giant cells have been shown to migrate through the insert ahead of smaller cell types (Hemberger, et al. 2004). In vivo, altered patterns of trophoblast invasion have been reported in a rat model of maternal gestational obesity (Hayes, et al. 2014). We observed that after 6-12 hours in culture, relatively few cells had migrated to the lower surface of the membrane, however, after 36 hours in culture it was not possible to identify individual nuclei. Therefore, in order to characterise invasive and migratory phenotype, we assessed outgrowths after 18 and 24 hours in culture. In contrast to our findings of EPC outgrowth phenotype on Matrigel coated cover slips, we observed no

difference in EPC explant invasive characteristics, with respect to maternal diet, when assessed using transwell inserts. This difference could be accounted for by the fact that on cover slips, outgrowing cells can only migrate away radially and in a single plane from the central EPC, however, with transwell inserts cells can disperse to the lower surface and migrate in any direction resulting in more diffuse outgrowth patterns. As it was only possible to analyse the lower surface of the transwell insert, it was not possible to assess the proportions of cells remaining on the upper surface, or which may still be migrating through the membrane. As such, for future studies increasing the number of analytical time points, assessing for specific markers of secondary TGCs, determining gene and protein expression patterns within our outgrowths and/or assessing TGC development in vivo would all provide additional insight into the invasive characteristics of EPC outgrowths in response to maternal diet. In addition, as our outgrowths were cultured under ambient oxygen condition, as appose to the more physiological low oxygen tension observed *in utero,* we cannot rule out potential confounding effects on TGC phenotype in response to this disparity. As such, future *in vitro* studies will employ conditions more physiologically relevant to mimic better those observed in utero.

It would be anticipated that any adaptive mechanisms initiated within LPD pre-implantation embryos would also be induced within Emb-LPD embryos. It was of interest to observe significant differences in outgrowth phenotype between LPD and Emb-LPD EPCs cultured on cover slips. Analysis of changes in outgrowth proportions over time did however, reveal that LPD and Emb-LPD explants behaved in an identical manner, reducing the relative proportion of the EPC and increasing the relative proportion of secondary TGC's. This was in stark contrast to NPD outgrowths which remained proportionally unchanged over the same period. As discussed earlier, we proposed that maternal LPD induces nutrient retrieval mechanisms within the extraembryonic lineages of the developing embryo. Therefore, maternal LPD may induce the blastocyst to invest disproportionately into the developing EPC post-implantation. If the maternal diet remains sub-

optimal then the adaptive investment increases rates of cell division and nutrient uptake in order to maintain fetal development under conditions of reduced nutrient availability. However, when maternal NPD is restored at implantation (Emb-LPD), rates of trophoblast cell division are unaltered, but the programmed enhanced nutrient uptake adaptations result in increased fetal growth.

The development and size of the late gestation placenta is directly linked to nutrient transport capacity and fetal growth. Placental morphology, thickness, fetal-placental blood flow and the expression and function of nutrient transporters also influence fetal growth and development (Salafia, et al. 2007). In addition to the placenta, the visceral yolk sac provides the developing fetus with a constant supply of amino acids through the breakdown of maternal proteins throughout gestation. Therefore, we determined whether changes in post-implantation trophoblast phenotype impacted on fetal, placental and yolk sac development in late gestation (E17). Our analysis revealed elevated fetal growth in offspring from Emb-LPD dams, mirroring our previous findings of elevated Emb-LPD offspring weight at birth and of late gestation fetuses derived from LPD blastocysts transferred into NPD dams (Watkins, et al. 2008). In addition, we observed a significantly elevated fetal:yolk sac weight ratio in Emb-LPD fetuses when compared with NPD and LPD fetuses. Maternal LPD in the mouse has been shown to enhance nutrient uptake activity within the blastocyst trophectoderm and embryoid body primitive endoderm (Sun, et al. 2014) and elevate visceral yolk sac endocytosis in late gestation (Watkins, et al. 2008). Therefore, the enhanced fetal growth observed in Emb-LPD offspring could be programmed in part through increased delivery of essential nutrition by the yolk sac during gestation. Conversely, fetuses from LPD dams displayed comparable fetal weight but with a significantly reduced placental weight. The significantly increased Emb-LPD fetal weight, and decreased LPD placental weight resulted in significantly elevated fetal:placental weights ratio in both LPD and Emb-LPD fetuses. The fetal:placental ratio is seen as an indicator of placental nutrient transport capacity, with an increased ratio considered a

sign of enhanced placental efficiency (Fowden, et al. 2009). As discussed above, in response to maintained maternal LPD, it may be more metabolically favourable to establish placentation earlier and minimise placental growth in later gestation when maternal resources are constrained. However, this adaptation may then result in altered placental function and transport, having important consequences for offspring growth and adult health. Maternal LPD in rats has been shown to result in the down regulation of placental amino acid transporters ahead of development of intrauterine fetal growth restriction (Jansson, et al. 2006, Malandro, et al. 1996). Sferruzzi-Perri, et al. (2013) showed that a maternal obesogenic diet reduced fetal and placental growth, but enhanced placental glucose and amino acid transport, as well as expression of fatty acid transporters and metabolic signalling pathway mediators. The molecular regulation of placental nutrient transport is believed to be co-ordinated through mTORC1, acting as a central nutrient sensor orchestrating fetal demand with maternal supply (Jansson, et al. 2012). Maternal gestational nutrient restriction has been shown to decrease placental mTORC1 activity in the baboon (Kavitha, et al. 2014), human IUGR pregnancies (Roos, et al. 2007, Yung, et al. 2008) and in response to rodent LPD (Jansson, et al. 2006, Rosario, et al. 2011). In addition, circulating levels of insulin and branched chain amino acids, activators of mTORC1, are altered in models of maternal dietary induced obesity (Gaccioli, et al. 2013, Lager, et al. 2014). Therefore, we investigated the expression of key downstream targets of mTORC1 and their phosphorylation status in placentas from LPD and Emb-LPD dams. Here, we observed minimal impacts of maternal diet on signalling through the mTORC1 pathway as assessed by the total and phosphorylated levels of the initiation factor eIF4E and S6 ribosomal protein in either placental or yolk sac tissues. Whilst significant changes in maternal metabolite and growth factor levels have been shown at the time of implantation in response to maternal LPD (Eckert, et al. 2012, Kwong, et al. 2000), the demonstration of late gestation maternal autophagy in rat dams fed LPD (Wang, et al. 2014) raises the possibility that maternal nutritional status stabilises after several days of LPD, resulting in the similar levels of mTOC1 signalling observed in the present study. In addition, as physiological exchange between maternal and fetal circulations occurs within

the labyrinthine zone of the placenta, our analysis of mTOR signalling within the whole placenta may have masked zone-specific differences. Finally, the placenta may augment other mechanisms independently of mTOR to modify nutrient transport, thus resulting in similar levels of mTOR signalling, but still affecting fetal development. For example, in nutrient restricted sheep at mid-gestation, a reduction in fetal growth is observed with increased AMPK and ERK1/2 activity but with no change in mTOR and Akt signalling (Ma et al., 2011).

Taken together, our results suggest that maternal LPD programs post-implantation trophoblast growth and phenotype in order to maintain embryonic and fetal development within a sub-optimal nutritional environment. In late gestation, the maintenance of maternal LPD results in a significantly smaller placenta but with comparable fetal weight, suggestive of enhanced placental efficiency and transport. However, these adaptive mechanisms, whilst supporting offspring development to birth and reproductive age, become maladaptive and predispose offspring to adult-onset disease (Watkins, et al. 2008). In contrast, maternal Emb-LPD does not affect early post-implantation trophoblast spreading and cell number, due potentially to the restoration of maternal nutrition to optimal (NPD) levels post-implantation. However, the induction of enhanced nutrient uptake capacity, programmed within the blastocyst in response to preimplantation LPD, results in elevated fetal growth in late gestation, also inducing adult cardiovascular and metabolic disease (Watkins, et al. 2008). These data add new insight into the sensitivity of the developing embryo in response to maternal nutrition at the time of embryo implantation, for the programming of offspring growth and subsequent health.

Declaration of interests

All authors declare that there are no conflicts of interest that could be perceived as prejudicing the impartiality of the research reported.

Funding

This work was supported through awards from the Biotechnology and Biological Sciences Research Council [BB/F007450/1; BB/I001840/1] to TPF.

Acknowledgements

We thank staff from the University of Southampton Biomedical Research Facility for animal provision and maintenance .

References

Adamson, SL, Y Lu, KJ Whiteley, D Holmyard, M Hemberger, C Pfarrer, and JC Cross 2002 Interactions between trophoblast cells and the maternal and fetal circulation in the mouse placenta. *Dev Biol* **250** 358-373.

Armitage, JA, IY Khan, PD Taylor, PW Nathanielsz, and L Poston 2004 Developmental programming of the metabolic syndrome by maternal nutritional imbalance: how strong is the evidence from experimental models in mammals? *J Physiol* **561** 355-377.

Auman, HJ, T Nottoli, O Lakiza, Q Winger, S Donaldson, and T Williams 2002 Transcription factor AP-2gamma is essential in the extra-embryonic lineages for early postimplantation development. *Development* **129** 2733-2747.

Bauer, S, J Pollheimer, J Hartmann, P Husslein, JD Aplin, and M Knofler 2004 Tumor necrosis factor-alpha inhibits trophoblast migration through elevation of plasminogen activator inhibitor-1 in first-trimester villous explant cultures. *J Clin Endocrinol Metab* **89** 812-822.

Bevilacqua, EM, and PA Abrahamsohn 1988 Ultrastructure of trophoblast giant cell transformation during the invasive stage of implantation of the mouse embryo. *J Morphol* **198** 341-351.

Brown, DG, VN Warren, P Pahlsson, and SJ Kimber 1993 Carbohydrate antigen expression in murine embryonic stem cells and embryos. I. Lacto and neo-lacto determinants. *Histochem J* **25** 452-463.

Caluwaerts, S, R Pijnenborg, C Luyten, and FA Van Assche 2000 Growth characteristics of diabetic rat ectoplacental cones in vivo and in vitro. *Diabetologia* **43** 939-945.

Centrella, M, E Canalis, TL McCarthy, AF Stewart, JJ Orloff, and KL Insogna 1989 Parathyroid hormone-related protein modulates the effect of transforming growth factor-beta on deoxyribonucleic acid and collagen synthesis in fetal rat bone cells. *Endocrinology* **125** 199-208.

Chen, PY, A Ganguly, L Rubbi, LD Orozco, M Morselli, D Ashraf, A Jaroszewicz, S Feng, SE Jacobsen, A Nakano, SU Devaskar, and M Pellegrini 2013 Intrauterine calorie restriction affects placental DNA methylation and gene expression. *Physiol Genomics* **45** 565-576.

Coan, PM, OR Vaughan, J McCarthy, C Mactier, GJ Burton, M Constancia, and AL Fowden 2011 Dietary composition programmes placental phenotype in mice. *J Physiol* **589** 3659-3670.

Dowling, RJ, I Topisirovic, BD Fonseca, and N Sonenberg 2010 Dissecting the role of mTOR: lessons from mTOR inhibitors. *Biochim Biophys Acta* **1804** 433-439.

Eckert, JJ, R Porter, AJ Watkins, E Burt, S Brooks, HJ Leese, PG Humpherson, IT Cameron, and TP Fleming 2012 Metabolic induction and early responses of mouse blastocyst developmental programming following maternal low protein diet affecting life-long health. *PLoS One* **7** e52791.

El-Hashash, AH, and SJ Kimber 2004 Trophoblast differentiation in vitro: establishment and characterisation of a serum-free culture model for murine secondary trophoblast giant cells. *Reproduction* **128** 53-71.

El-Hashash, AH, P Esbrit, SJ Kimber 2005 PTHrP promotes murine secondary trophoblast giant cell differentiation through induction of endocycle, upregulation of giant-cell-promoting transcription factors and suppression of other trophoblast cell types. *Differentiation*. **73** 154-74.

El-Hashash, AH, D Warburton, and SJ Kimber 2010 Genes and signals regulating murine trophoblast cell development. *Mech Dev* **127** 1-20.

Fowden, AL, AN Sferruzzi-Perri, PM Coan, M Constancia, and GJ Burton 2009 Placental efficiency and adaptation: endocrine regulation. *J Physiol* **587** 3459-3472.

Gabory, A, L Ferry, I Fajardy, L Jouneau, JD Gothie, A Vige, C Fleur, S Mayeur, C Gallou-Kabani, MS Gross, L Attig, A Vambergue, J Lesage, B Reusens, D Vieau, C Remacle, JP Jais, and C Junien 2012 Maternal diets trigger sex-specific divergent trajectories of gene expression and epigenetic systems in mouse placenta. *PLoS One* **7** e47986.

Gaccioli, F, V White, E Capobianco, TL Powell, A Jawerbaum, and T Jansson 2013 Maternal overweight induced by a diet with high content of saturated fat activates placental mTOR and eIF2alpha signaling and increases fetal growth in rats. *Biol Reprod* **89** 96.

Georgiades, P, AC Ferguson-Smith, and GJ Burton 2002 Comparative developmental anatomy of the murine and human definitive placentae. *Placenta* **23** 3-19.

Gheorghe, CP, R Goyal, JD Holweger, and LD Longo 2009 Placental gene expression responses to maternal protein restriction in the mouse. *Placenta* **30** 411-417.

Hanson, MA, and PD Gluckman 2014 Early Developmental Conditioning of Later Health and Disease: Physiology or Pathophysiology? *Physiol Rev* **94** 1027-1076.

Hayes, EK, DR Tessier, ME Percival, AC Holloway, JJ Petrik, A Gruslin, and S Raha 2014 Trophoblast invasion and blood vessel remodeling are altered in a rat model of lifelong maternal obesity. *Reprod Sci* **21** 648-657.

Hemberger, M, M Hughes, and JC Cross 2004 Trophoblast stem cells differentiate in vitro into invasive trophoblast giant cells. *Dev Biol* **271** 362-371.

Jansson, N, J Pettersson, A Haafiz, A Ericsson, I Palmberg, M Tranberg, V Ganapathy, TL Powell, and T Jansson 2006 Down-regulation of placental transport of amino acids precedes the development of intrauterine growth restriction in rats fed a low protein diet. *J Physiol* **576** 935-946.

Jansson, T, IL Aye, and DC Goberdhan 2012 The emerging role of mTORC1 signaling in placental nutrient-sensing. *Placenta* **33 Suppl 2** e23-29.

Jovanovic, M, I Stefanoska, L Radojcic, and L Vicovac 2010 Interleukin-8 (CXCL8) stimulates trophoblast cell migration and invasion by increasing levels of matrix metalloproteinase (MMP)2 and MMP9 and integrins alpha5 and beta1. *Reproduction* **139** 789-798.

Kavitha, JV, FJ Rosario, MJ Nijland, TJ McDonald, G Wu, Y Kanai, TL Powell, PW Nathanielsz, and T Jansson 2014 Down-regulation of placental mTOR, insulin/IGF-I signaling, and nutrient transporters in response to maternal nutrient restriction in the baboon. *FASEB J* **28** 1294-1305.

Kim, DW, SL Young, DR Grattan, and CL Jasoni 2014 Obesity during pregnancy disrupts placental morphology, cell proliferation, and inflammation in a sex-specific manner across gestation in the mouse. *Biol Reprod* **90** 130.

Kim, E 2009 Mechanisms of amino acid sensing in mTOR signaling pathway. *Nutr Res Pract* **3** 64-71.

Kwong, WY, AE Wild, P Roberts, AC Willis, and TP Fleming 2000 Maternal undernutrition during the preimplantation period of rat development causes blastocyst abnormalities and programming of postnatal hypertension. *Development* **127** 4195-4202.

Lager, S, AM Samulesson, PD Taylor, L Poston, TL Powell, and T Jansson 2014 Diet-induced obesity in mice reduces placental efficiency and inhibits placental mTOR signaling. *Physiol Rep* **2** e00242.

Ma, Y,MJ Zhu, AB Uthlaut, MJ Nijland, PW Nathanielsz, BW Hess, and SP Ford 2011 Upregulation of growth signaling and nutrient transporters in cotyledons of early to mid-gestational nutrient restricted ewes. *Placenta* **32** 255-63.

Malandro, MS, MJ Beveridge, MS Kilberg, and DA Novak 1996 Effect of low-protein diet-induced intrauterine growth retardation on rat placental amino acid transport. *Am J Physiol* **271** C295-303.

O'Brien, PJ, H Koi, S Parry, LF Brass, JF Strauss, 3rd, LP Wang, JE Tomaszewski, and LK Christenson 2003 Thrombin receptors and protease-activated receptor-2 in human placentation: receptor activation mediates extravillous trophoblast invasion in vitro. *Am J Pathol* **163** 1245-1254.

688

689 **Pavan, L, A Hermouet, V Tsatsaris, P Therond, T Sawamura, D Evain-Brion, and T Fournier**
690 2004 Lipids from oxidized low-density lipoprotein modulate human trophoblast invasion:
691 involvement of nuclear liver X receptors. *Endocrinology* **145** 4583-4591.

692

693 **Roos, S, N Jansson, I Palmberg, K Saljo, TL Powell, and T Jansson** 2007 Mammalian target of
694 rapamycin in the human placenta regulates leucine transport and is down-regulated in restricted
695 fetal growth. *J Physiol* **582** 449-459.

696

697 **Rosario, FJ, N Jansson, Y Kanai, PD Prasad, TL Powell, and T Jansson** 2011 Maternal protein
698 restriction in the rat inhibits placental insulin, mTOR, and STAT3 signaling and down-regulates
699 placental amino acid transporters. *Endocrinology* **152** 1119-1129.

700

701 **Rossant, J, and JC Cross** 2001 Placental development: lessons from mouse mutants. *Nat Rev*
702 *Genet* **2** 538-548.

703

704 **Salafia, CM, J Zhang, RK Miller, AK Charles, P Shrout, and W Sun** 2007 Placental growth
705 patterns affect birth weight for given placental weight. *Birth Defects Res A Clin Mol Teratol* **79**
706 281-288.

707

708 **Sato, Y, H Fujiwara, T Higuchi, S Yoshioka, K Tatsumi, M Maeda, and S Fujii** 2002
709 Involvement of dipeptidyl peptidase IV in extravillous trophoblast invasion and differentiation. *J*
710 *Clin Endocrinol Metab* **87** 4287-4296.

711

Scott, IC, L Anson-Cartwright, P Riley, D Reda, and JC Cross 2000 The HAND1 basic helix-loop-helix transcription factor regulates trophoblast differentiation via multiple mechanisms. *Mol Cell Biol* **20** 530-541.

Sferruzzi-Perri, AN, OR Vaughan, M Haro, WN Cooper, B Musial, M Charalambous, D Pestana, S Ayyar, AC Ferguson-Smith, GJ Burton, M Constancia, and AL Fowden 2013 An obesogenic diet during mouse pregnancy modifies maternal nutrient partitioning and the fetal growth trajectory. *FASEB J* **27** 3928-3937.

Simmons, DG, and JC Cross 2005 Determinants of trophoblast lineage and cell subtype specification in the mouse placenta. *Dev Biol* **284** 12-24.

Simmons, DG, AL Fortier, and JC Cross 2007 Diverse subtypes and developmental origins of trophoblast giant cells in the mouse placenta. *Dev Biol* **304** 567-578.

Soares, MJ, T Konno, and SM Alam 2007 The prolactin family: effectors of pregnancy-dependent adaptations. *Trends Endocrinol Metab* **18** 114-121.

Staff, AC, T Ranheim, T Henriksen, and B Halvorsen 2000 8-Iso-prostaglandin f(2alpha) reduces trophoblast invasion and matrix metalloproteinase activity. *Hypertension* **35** 1307-1313.

Sun, C, MA Velazquez, S Marfy-Smith, B Sheth, A Cox, DA Johnston, N Smyth, and TP Fleming 2014 Mouse early extra-embryonic lineages activate compensatory endocytosis in response to poor maternal nutrition. *Development* **141** 1140-1150.

Vaughan, OR, AN Sferruzzi-Perri, PM Coan, and AL Fowden 2011 Environmental regulation of placental phenotype: implications for fetal growth. *Reprod Fertil Dev* **24** 80-96.

Wang, H, D Zhou, and Y-X Pan 2014 Low protein diet during gestation and lactation induces autophagy-related gene LC3 in the liver of rat dams (737.5). *The FASEB Journal* **28**.

Watkins, AJ, ES Lucas, C Torrens, JK Cleal, L Green, C Osmond, JJ Eckert, WP Gray, MA Hanson, and TP Fleming 2010 Maternal low-protein diet during mouse pre-implantation development induces vascular dysfunction and altered renin-angiotensin-system homeostasis in the offspring. *Br J Nutr* **103** 1762-1770.

Watkins, AJ, ES Lucas, A Wilkins, FR Cagampang, and TP Fleming 2011 Maternal periconceptional and gestational low protein diet affects mouse offspring growth, cardiovascular and adipose phenotype at 1 year of age. *PLoS One* **6** e28745.

Watkins, AJ, E Ursell, R Panton, T Papenbrock, L Hollis, C Cunningham, A Wilkins, VH Perry, B Sheth, WY Kwong, JJ Eckert, AE Wild, MA Hanson, C Osmond, and TP Fleming 2008 Adaptive responses by mouse early embryos to maternal diet protect fetal growth but predispose to adult onset disease. *Biol Reprod* **78** 299-306.

Xu, G, MJ Guimond, C Chakraborty, and PK Lala 2002 Control of proliferation, migration, and invasiveness of human extravillous trophoblast by decorin, a decidual product. *Biol Reprod* **67** 681-689.

Yung, HW, S Calabrese, D Hynx, BA Hemmings, I Cetin, DS Charnock-Jones, and GJ Burton 2008 Evidence of placental translation inhibition and endoplasmic reticulum stress in the etiology of human intrauterine growth restriction. *Am J Pathol* **173** 451-462.

Zorn, TM, M Zuniga, E Madrid, R Tostes, Z Fortes, F Giachini, and S San Martin 2011 Maternal diabetes affects cell proliferation in developing rat placenta. *Histol Histopathol* **26** 1049-1056.

771 **Figure legends**

772 **Figure 1.** Representative images of E8.5 mouse EPC explant outgrowths grown on Matrigel coated
773 cover slips. (a) Inverted brightfield image taken on a Leica DSM 5000 microscope after 24 hours
774 showing small, densely packed cells and with elongated nuclei surrounding the central EPC (arrow
775 head) and larger more widely spaced cells with rounded nuclei (arrow) at the periphery (shown at
776 higher magnification in d-f) , or (b) top-illuminated brightfield image taken on a Zeiss Stemi SV11
777 stereomicroscope after 48 hours in culture. (c) Whole image of DAPI stained outgrowth after 48
778 hours in culture. (d) Magnified section of an outgrowth showing the central EPC (*), small, closely
779 associated 'proliferative' (‡) and peripheral 'secondary' (arrow) trophoblast giant cells in
780 outgrowths after 48 hours in culture. (e) Phase contrast image of peripheral trophoblast giant cells
781 (arrow) identifying a monolayer of large, multinucleated cells after 48 hours of culture at the
782 periphery of the 'proliferative' (‡) cells. (f) Immunofluorescence image stained for alpha tubulin,
783 showing multinucleated peripheral trophoblast giant cells (arrow) after 48 hours of culture with
784 proliferative layer (‡) and central EPC (*) shown on right.

785

786 **Figure 2**. (a-c) Example E8.5 mouse EPC explant outgrowth analysis using Volocity software to
787 determine EPC area (highlighted in red in a) and distance of the furthest nucleus from the EPC
788 centre (solid white line from the centre of the superimposed square in b) and the combined area of
789 the EPC and proliferative cells (highlighted in red) in (c). The area of the secondary TGCs was
790 determined as the areas of the entire outgrowth minus the combined area of the EPC and
791 proliferative TGCs. (d-k) Mean EPC outgrowth measurements from NPD (white bars), LPD (black
792 bars) and Emb-LPD (grey bars) explants grown on Matrigel coated cover slips after 24 and 48
793 hours. n = 10-14 outgrowths taken from 6-8 separate females per diet per culture time and treatment
794 group. Error bars are S.E.M. Different letters denote statistical significance between groups at
795 $P<0.05$.

796

Figure 3. (a) Mean % composition of NPD (white bars), LPD (black bars) and Emb-LPD (grey bars) explants grown on Matrigel coated cover slips after 24 and (b) 48 hours. (c) Mean change in outgrowth composition between 24 and 48 hours of culture. n = 10-14 outgrowths per culture time and treatment group, taken from 6-8 separate females per diet. Error bars are S.E.M. Different letters denote statistical significance between groups at $P<0.05$.

Figure 4. (a) High magnification image of a DAPI stained Transwell invasion chamber showing cells migrating (arrows) though the 8 µm membrane pores (arrow head) after 6 hours in culture. (b) Lower magnification image of a DAPI stained Transwell invasion chamber after 6, (c) 12 and (d) 18 hours of culture. (e) Haemotoxylin stained outgrowth after 18 hours of culture. (f) Magnified section showing large, multinucleated peripheral cells (arrows) and 8 µm pores (arrow heads). (g-k) Mean EPC outgrowth measurement from NPD (white bars), LPD (black bars) and Emb-LPD (grey bars) explants grown on Matrigel invasion transwell inserts after 18 and 24 hours. n = 6-7 outgrowths per culture time and treatment group, taken from 6-7 separate females per diet. Error bars are S.E.M Different letters denote statistical significance between groups at $P<0.05$.

Figure 5. Representative immunoblots in E17 (a, c) placenta and (e, g) yolk sac tissues for mTORC1 downstream targets of total and phosphorylated (a, e) 4E-BP1 and (c, g) S6 protein levels and the reference protein α-tubulin. Individual blot lanes include molecular weight markers (far left) and samples of NPD (N), LPD (L) and Emb-LPD (E) tissues (20 µg total protein per lane) and loading control (LC). Mean integrated density values for total and phosphorylated levels of (b, f) 4E-BP1and (d, h) S6 ribosomal protein in NPD (white bars), LPD (black bars) and Emb-LPD (grey bars) E17 (b, d) placental and (f, h) yolk sac tissues normalised to α-tubulin. n = 8 samples per treatment, all from separate litters. Error values are S.E.M.

823 **Table 1**. Mean weights of concepti and fetal tissues from NPD, LPD and Emb-LPD fed mouse

824 dams at day 17 of gestation.

825

	Diet		
Tissue	**NPD**	**LPD**	**Emb-LPD**
Conceptus (mg)	1261.7 ± 15.9 [a]	1227.6 ± 18.5 [a]	1324.2 ± 18.2 [b]
Fetus (mg)	941.2 ± 8.6 [a]	943.4 ± 9.4 [a]	1039.5 ± 9.3 [b]
Placenta (mg)	169.2± 2.5 [a]	150.1 ± 1.9 [b]	159.7 ± 2.2 [a]
Yolk sac (mg)	82.2 ± 1.6	87.6 ± 1.6	83.03 ± 2.0
Fetal:Placental	5.74 ± 0.09 [a]	6.40 ± 0.09 [b]	6.64 ± 0.09 [b]
Fetal:Yolk sac	12.37± 0.32 [a]	11.46 ± 0.29 [a]	13.61 ± 0.38 [b]

826

827

828 n = 13-14 dams per treatment group. Error values are S.E.M. Different letters denote statistical

829 significance at $P<0.05$.

830

831

832 **Figure 1**

833

834

835

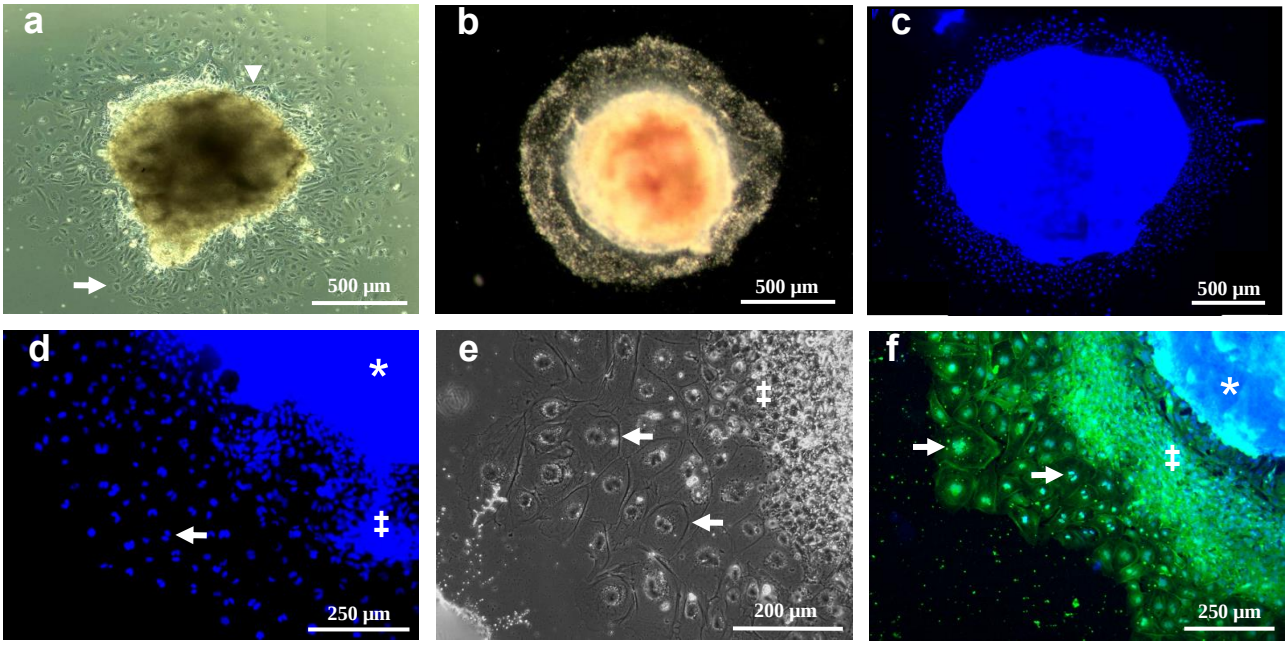

Figure 2

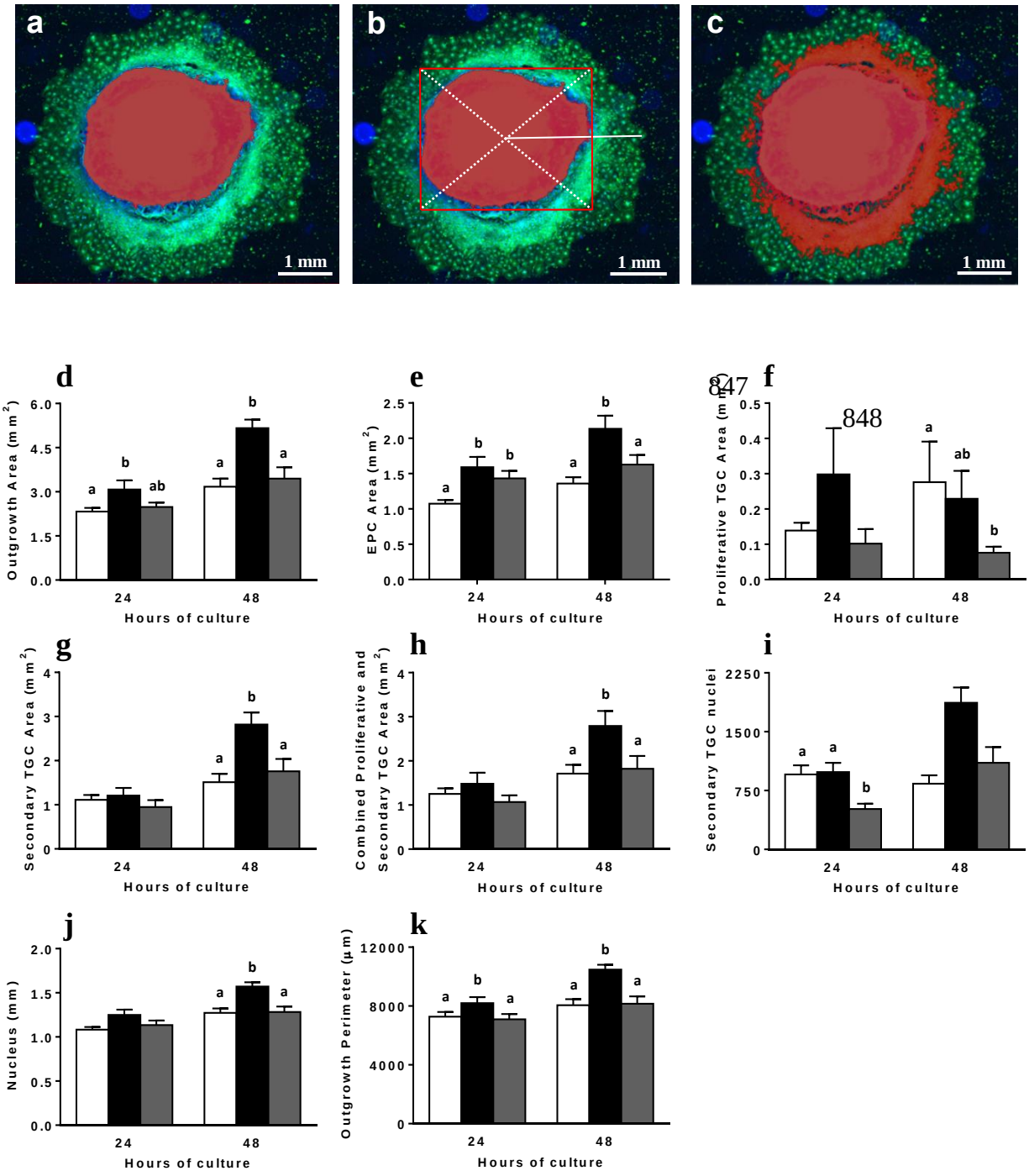
a
b
c
1 mm
1 mm
1 mm
d
Outgrowth Area (mm²)
Hours of culture
e
EPC Area (mm²)
Hours of culture
f
Proliferative TGC Area (m
Hours of culture
g
Secondary TGC Area (mm²)
Hours of culture
h
Combined Proliferative and Secondary TGC Area (mm²)
Hours of culture
i
Secondary TGC nuclei
Hours of culture
j
Distance of Furthest Nucleus (mm)
Hours of culture
k
Outgrowth Perimeter (µm)
Hours of culture
24
48

Figure 3

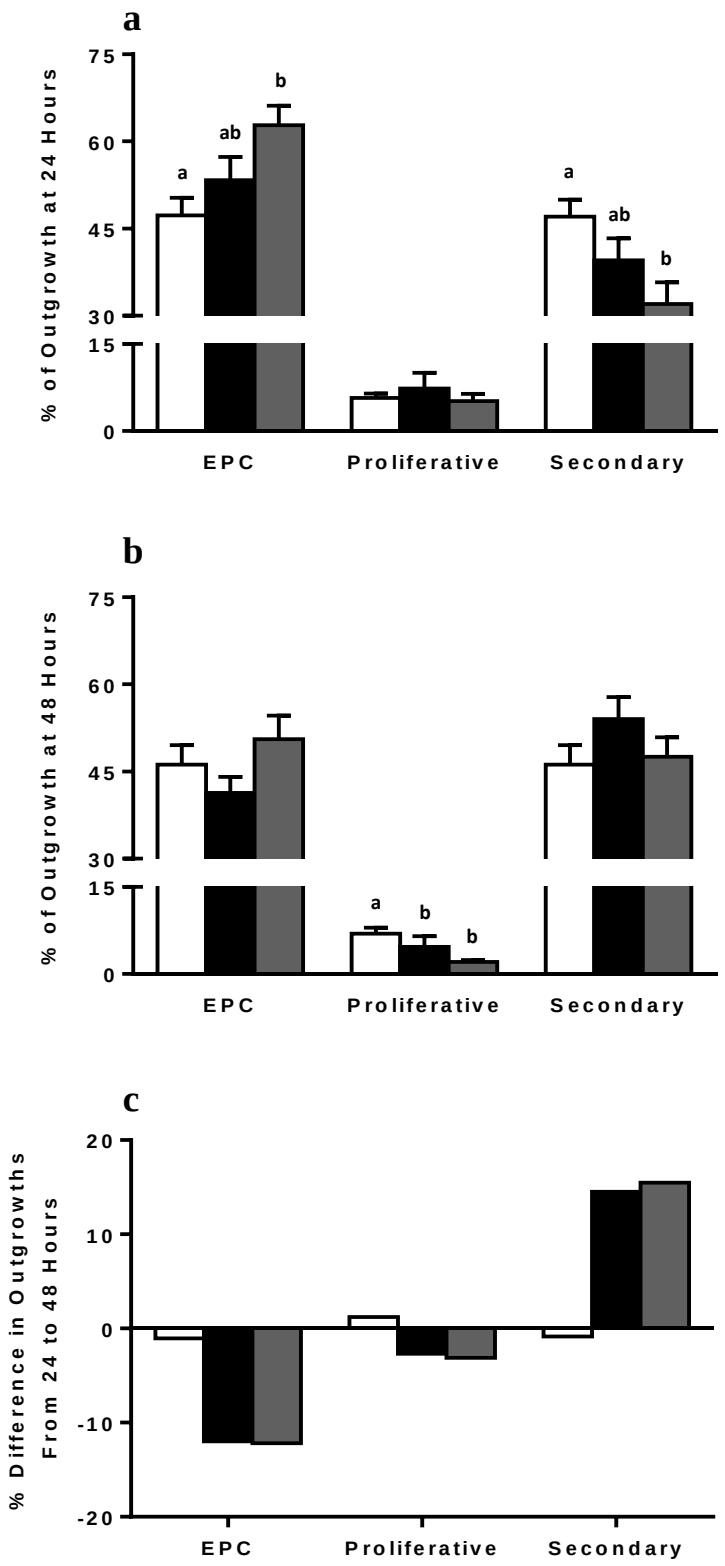
a
% of Outgrowth at 24 Hours
75
60
45
30
15
0
a
ab
b
a
ab
b
EPC
Proliferative
Secondary
b
% of Outgrowth at 48 Hours
75
60
45
30
15
0
a
b
b
EPC
Proliferative
Secondary
c
% Difference in Outgrowths From 24 to 48 Hours
20
10
0
-10
-20
EPC
Proliferative
Secondary

Figure 4

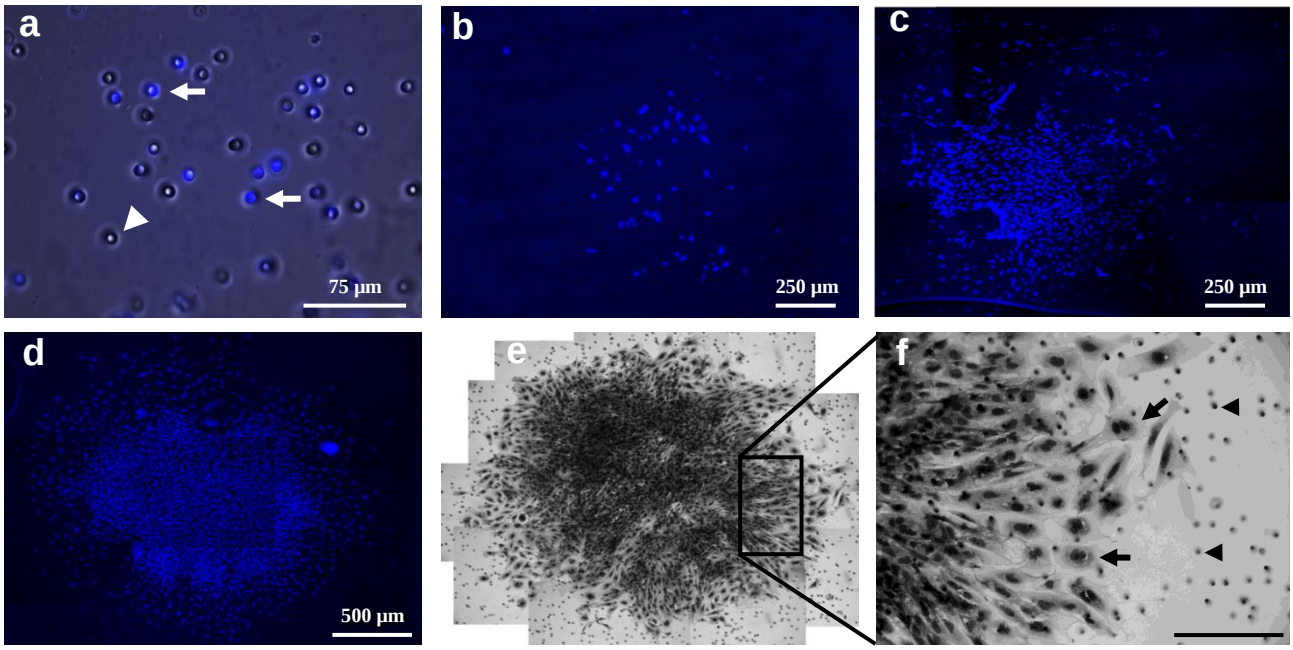
a
75 µm
b
250 µm
c
250 µm
d
500 µm
e
f

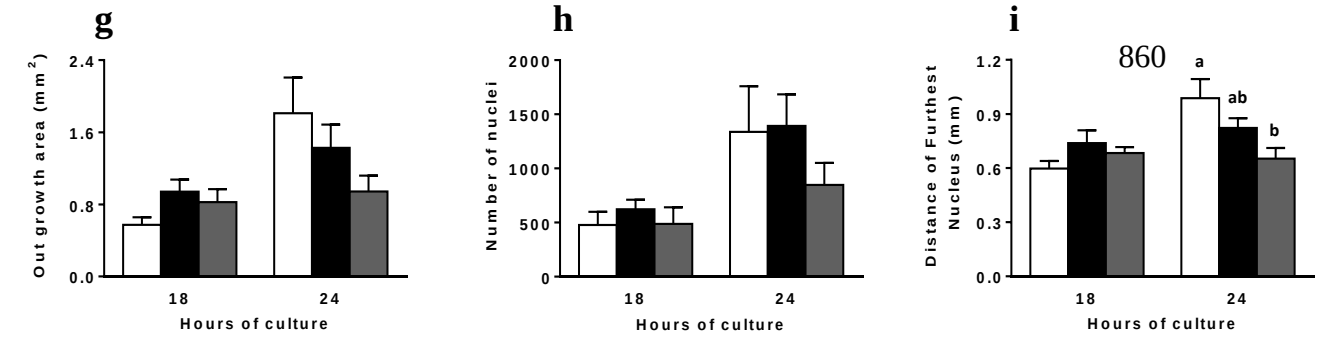
g
Out growth area (mm2)
2.4
1.6
0.8
0.0
18
24
Hours of culture
h
Number of nuclei
2000
1500
1000
500
0
18
24
Hours of culture
i
Distance of Furthest Nucleus (mm)
1.2
0.9
0.6
0.3
0.0
a
ab
b
18
24
Hours of culture

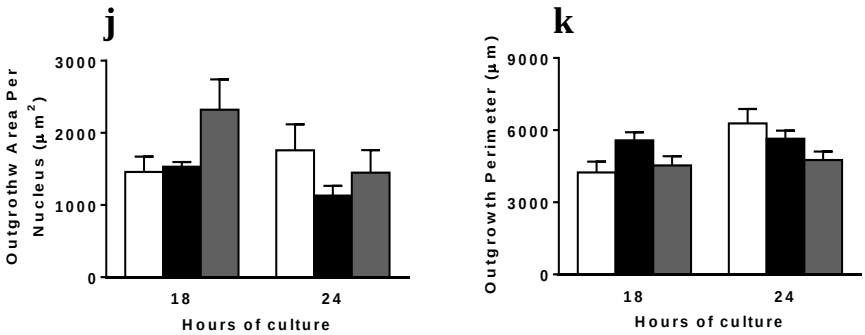
j
Outgrothw Area Per Nucleus (µm2)
3000
2000
1000
0
18
24
Hours of culture
k
Outgrowth Perimeter (µm)
9000
6000
3000
0
18
24
Hours of culture

Figure 5

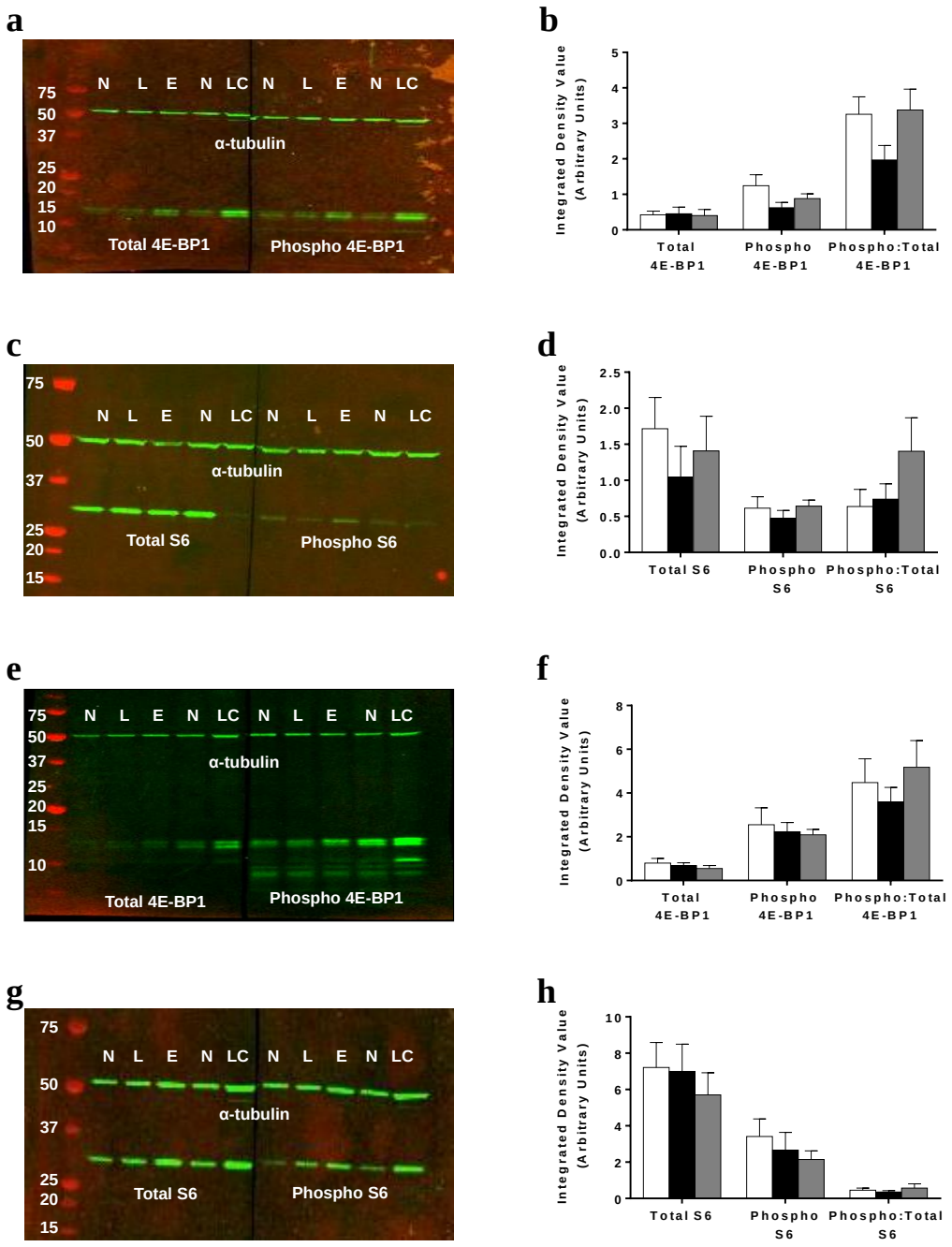
a
N L E N LC N L E N LC
75
50
37
25
20
15
10
α-tubulin
Total 4E-BP1
Phospho 4E-BP1
b
Integrated Density Value (Arbitrary Units)
5
4
3
2
1
0
Total 4E-BP1
Phospho 4E-BP1
Phospho:Total 4E-BP1
c
N L E N LC N L E N LC
75
50
37
25
20
15
α-tubulin
Total S6
Phospho S6
d
Integrated Density Value (Arbitrary Units)
2.5
2.0
1.5
1.0
0.5
0.0
Total S6
Phospho S6
Phospho:Total S6
e
N L E N LC N L E N LC
75
50
37
25
20
15
10
α-tubulin
Total 4E-BP1
Phospho 4E-BP1
f
Integrated Density Value (Arbitrary Units)
8
6
4
2
0
Total 4E-BP1
Phospho 4E-BP1
Phospho:Total 4E-BP1
g
N L E N LC N L E N LC
75
50
37
25
20
15
α-tubulin
Total S6
Phospho S6
h
Integrated Density Value (Arbitrary Units)
10
8
6
4
2
0
Total S6
Phospho S6
Phospho:Total S6

863